Lewis Acids

DOI: 10.1002/anie.201106242

Sensing of Aqueous Fluoride Anions by Cationic Stibine–Palladium Complexes**

*Casey R. Wade, Iou-Sheng Ke, and François P. Gabbaï**

The advent of triarylboranes as anion receptors has led to a number of positive developments, including the discovery of water-compatible sensors for the potentially toxic fluoride anion.[1] The success of this approach lies in the ability of triarylboranes to form a covalent bond with the anionic guest (case A) and respond to its presence with a change of the photophysical properties. As part of our interest in fundamental aspects of main-group chemistry, we recently questioned whether alternative fluoride anion sensing platforms based on main-group Lewis acids could be envisaged.[2] With this idea in mind, we were drawn by the reported ability of Ph_4Sb^+ to react with fluoride anions in CCl_4/H_2O and generate the corresponding fluorostiborane Ph_4SbF (case B).[3] While this observed reactivity attests to the strength of the Sb–F bond, the absence of major photophysical changes during the formation of the fluorostiborane limits the development of a fluoride anion sensing application.

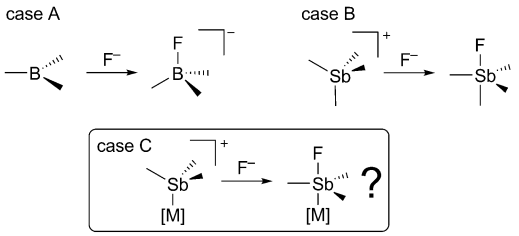

Cationic triarylstibine/transition-metal complexes have been reported previously.[4] Like stibonium ions, such species possess a four-coordinate antimony atom. On the basis of this simple structural analogy, we speculated that: 1) The antimony atom of such complexes may be reactive toward fluoride ions. 2) The anion, which binds at the antimony center, may affect the properties of the transition-metal center, thus leading to an easily detectable optical signal (case C). Herein, we report a series of results that provide an initial validation of this approach.

We decided to focus on a family of complexes in which the M–Sb bond is supported by auxiliary chelating ligands to prevent an anion-induced cleavage of the M–Sb bond. With this prerequisite in mind, we were drawn by the pioneering work of Baracco and McAuliffe, who described cationic palladium chloride complexes that feature the trisarsanylstibine ligand $(o\text{-}(Me_2As)C_6H_4)_3Sb$.[5] To enhance the stability of the complexes, we decided to revisit some aspects of this chemistry by using the trisphosphanylstibine ligand $(o\text{-}(Ph_2P)C_6H_4)_3Sb$ (referred to as L^3)[6] and its bisphosphanylphenyl analog $(o\text{-}(Ph_2P)C_6H_4)_2PhSb$ (referred to as L^2), which was synthesized for the purpose of this study. Reaction of these ligands with $[PdCl_2(cod)]$ (cod = 1,5-cyclooctadiene), and subsequent treatment with one equivalent of $NaBPh_4$ in CH_2Cl_2/EtOH, afforded the cationic palladium complexes $[L^3PdCl]^+$ (**1**$^+$) and $[L^2PdCl]^+$ (**2**$^+$) as the BPh_4^- salts in high yields (Scheme 1). The $^{31}P\{^1H\}$ NMR spectra in $CDCl_3$ show a

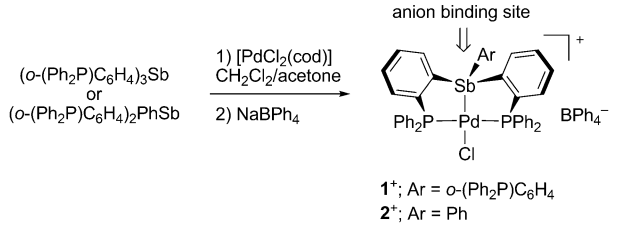

Scheme 1. Synthesis of [**1**]BPh_4 and [**2**]BPh_4.

single resonance at 39.72 ppm for **1**$^+$ and 53.81 ppm for **2**$^+$. The crystal structures of [**1**]BPh_4 and [**2**]BPh_4 show that the d^8 metal center in each complex adopts a square-planar geometry with the two coordinated phosphine arms in a trans arrangement (Figure 1).[7] In the case of [**1**]BPh_4, the Pd1–P3 distance of 4.15 Å indicates that the third phosphine arm is

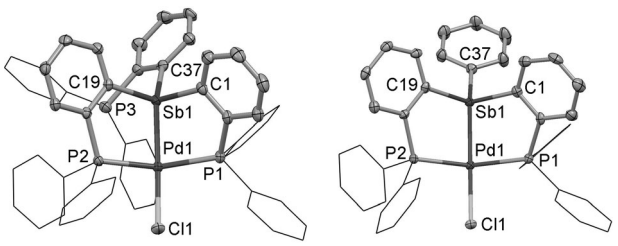

Figure 1. Crystal structures of [**1**]BPh_4 (left) and [**2**]BPh_4 (right). Thermal ellipsoids are drawn at the 50% probability level. Phenyl groups are drawn in wireframe, and hydrogen atoms and BPh_4^- anions are omitted for clarity. Pertinent metrical parameters can be found in the text.

[*] C. R. Wade, I.-S. Ke, Prof. Dr. F. P. Gabbaï
Department of Chemistry, Texas A&M University
College Station, TX 77843 (USA)
E-mail: francois@tamu.edu
Homepage: http://www.chem.tamu.edu/rgroup/gabbai/

[**] Financial support from the Welch Foundation (A-1423) and the National Science Foundation (CHE-0952912) is gratefully acknowledged.

Supporting information for this article is available on the WWW under http://dx.doi.org/10.1002/anie.201106242.

not coordinated to the palladium center, but rather sits above the square plane. The Pd1–Sb1 bond lengths of 2.4689(5) Å in [**1**]BPh_4 and 2.4816(6) in [**2**]BPh_4 are slightly shorter than those measured in the square-planar triarylstibine palladium complexes [*trans*-(*o*-$Tol_3Sb)_2PdCl_2$] (2.5658(3) Å; Tol = toluene) and [*trans*-$(Ph_3Sb)_2Pd(Ph)Cl$] (2.5568(5) Å), thus suggesting a tight coordination of the antimony ligand. These structural results indicate that the detection of a single resonance in the $^{31}P\{^1H\}$ NMR spectrum of $\mathbf{1}^+$ results from a rapid exchange of the phosphine arms on the NMR time scale. Accordingly, the ^1H NMR spectrum ($CDCl_3$) of $\mathbf{1}^+$ shows a single set of resonances corresponding to equivalent PPh_2 and *o*-C_6H_4 groups. Neither the $^{31}P\{^1H\}$ nor the ^1H NMR spectra of $\mathbf{1}^+$ showed any tendency toward decoalescence upon cooling to −50 °C in $CDCl_3$.

With these cationic complexes in hand, we sought to determine if they would exhibit a reactivity similar to tetraorganostibonium ions and form fluorostiboranes in the presence of fluoride ions.[3] To this end, solutions of [**1**]BPh_4 and [**2**]BPh_4 in CH_2Cl_2 were reacted with tetra-*n*-butylammonium fluoride (TBAF). While solutions of [**2**]BPh_4 and TBAF retained a pale-yellow color, an immediate color change from pale yellow to deep orange was observed in the case of [**1**]BPh_4 (Figure 2). These reactions were monitored by NMR spectroscopy in order to gain insight into their course. For the reaction of $\mathbf{1}^+$ with F^-, formation of the fluoride complex **1**-F was supported by detection of a doublet resonance in the $^{31}P\{^1H\}$ NMR spectrum of the reaction mixture (41.90 ppm, $^3J_{F\text{-}P} = 20.7$ Hz; Scheme 2). Consistent with this observation,

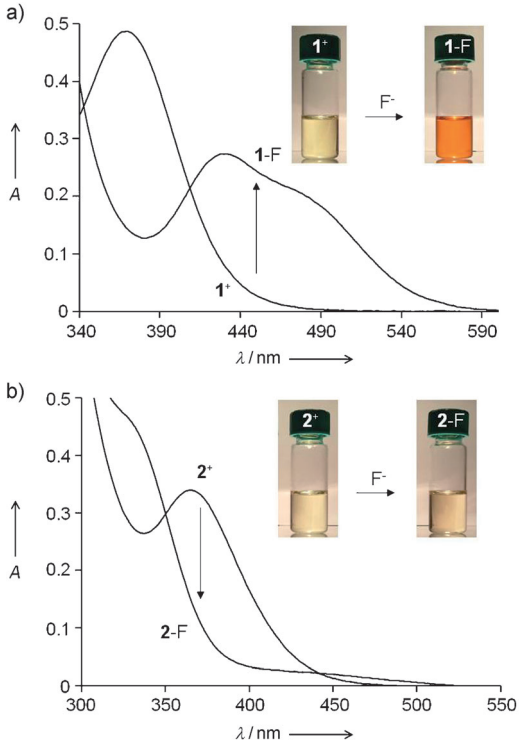

Figure 2. Absorption spectra of a) $\mathbf{1}^+$ and **1**-F (5.1×10^{-5} M) and b) $\mathbf{2}^+$ and **2**-F (4.8×10^{-5} M) in CH_2Cl_2. The pictures in the insets show the colorimetric response associated with the formation of the fluoride derivatives at a concentration of 5×10^{-4} M.

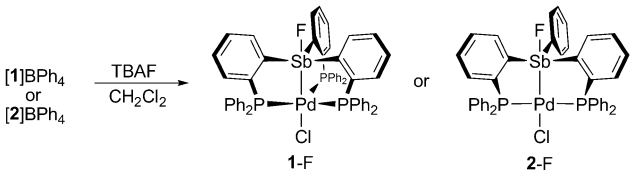

Scheme 2. Synthesis of **1**-F and **2**-F.

the ^{19}F NMR spectrum showed the appearance of a quartet resonance at −129.72 ppm ($^3J_{F\text{-}P} = 20.7$ Hz). Analogously, the ^{19}F and $^{31}P\{^1H\}$ NMR spectra of a mixture of $\mathbf{2}^+$ and F^- show resonances at −124.61 ppm and 64.06 ppm ($^3J_{F\text{-}P} = 26.7$ Hz), respectively, in agreement with the formation **2**-F.

In order to confirm that the fluoride anions in **1**-F and **2**-F are bound to antimony and not palladium, the structures of these complexes were determined by single-crystal X-ray diffraction.[7] In accordance with our original hypothesis, the structures show coordination of the fluoride anion to the antimony atom with Sb1–F1 bond lengths of 2.0320(19) Å for **1**-F and 2.0511(19) for **2**-F (Figure 3). These bond lengths are

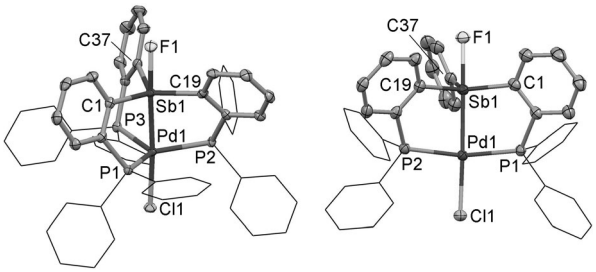

Figure 3. Crystal structures of **1**-F (left) and **2**-F (right). Thermal ellipsoids are drawn at the 50% probability level. Phenyl groups are drawn in wireframe and hydrogen atoms are omitted for clarity. Pertinent metrical parameters can be found in the text.

close to that observed in the fluorostiborane Ph_4SbF (2.0530(8) Å),[8] thus attesting to the presence of a strong interaction. Formation of these bonds induces a change of the coordination geometry of antimony from tetrahedral in $\mathbf{1}^+$ and $\mathbf{2}^+$ to trigonal-bipyramidal in **1**-F and **2**-F. These structural changes are reminiscent of those observed upon conversion of R_3SiF and R_3SnF species into the corresponding ate species $R_3SiF_2^-$ and $R_3SnF_2^-$, respectively.[2a,b] The major structural difference between **1**-F and **2**-F is found in the palladium coordination geometry, which is square-planar in **2**-F but trigonal-bipyramidal in **1**-F, with all three phosphines coordinated to the palladium center. The structural changes that accompany the conversion of $\mathbf{1}^+$ into **1**-F may be viewed as allosteric, with the coordination of the fluoride anion to the antimony atom modifying the denticity of the triphosphine–metal binding pocket. Finally, the Pd1–Sb1 bonds in the fluoride complexes (2.5721(7) Å for **1**-F and 2.5855(10) Å for **2**-F) are slightly longer than those measured in their cationic precursors (2.4689(5) Å for $\mathbf{1}^+$ and 2.4816(6) Å for $\mathbf{2}^+$), which is a trend that we assign to the change in the antimony coordination geometries. Both **1**-F and **2**-F constitute rare examples of stiboranyl complexes, which had not been observed with palladium prior to this work.[9] These com-

plexes can also be classified as metalla-metallatranes[10] and are especially reminiscent of the metalla-silatranes and metalla-stannatranes with hypervalent group 14 centers.[11] A density-functional theory (DFT) computational study carried out on $\mathbf{1}^+$ and **1**-F by using the ADF program (BP86/TZP with ZORA) followed by a Boys localization analysis indicates that the Sb–Pd bonding in these two compounds is polar covalent (Figure S7). This bonding characteristic is supported by the elevated contributions of both antimony and palladium atomic orbitals (Pd: 20.9%, Sb: 54.2% in $\mathbf{1}^+$; Pd: 43.7%, Sb: 27.4% in **1**-F) to the Sb–Pd bonding orbital. In the extreme of the dative-bond formalism, the Sb–Pd bond of these complexes can be viewed as switching from Sb:→Pd in $\mathbf{1}^+$ to Pd:→Sb in **1**-F. This change can be interpreted as an anion-induced umpolung of the Sb–Pd bond, reminiscent of that observed in a related gold system.[6b]

After we confirmed that the fluoride anion binds to the antimony center of these complexes, we turned our attention to the colorimetric response that accompanies the formation of **1**-F. In agreement with its pale-yellow color, the UV/Vis spectrum of $\mathbf{1}^+$ in CH_2Cl_2 shows an absorption band at $\lambda_{max} = 366$ nm, which tails off beyond 400 nm (Figure 2). This low-energy band is attributed to a combination of a metal-to-ligand charge transfer and ligand-centered transitions, which are typically observed for square-planar Pd complexes.[12] UV/Vis monitoring of the conversion of $\mathbf{1}^+$ into **1**-F upon incremental addition of fluoride anions shows a progressive quenching of the band at 366 nm, accompanied by the appearance of new absorption bands centered at 430 nm and 480 nm and spanning the 400–560 nm range. The appearance of these bands, which account for the deep-orange color of **1**-F, is assigned to ligand-field transitions ($d_{xy}, d_{x^2-y^2} \rightarrow d_{z^2}$ and $d_{xz}, d_{yz} \rightarrow d_{z^2}$) as previously reported for related trigonal-bipyramidal palladium complexes bearing tetradentate pnictogenyl ligands.[5,6,13] This interpretation is reinforced by the observation that $\mathbf{2}^+$, which lacks a third phosphine arm, retains a square-planar palladium center upon binding with the fluoride anion, and does not undergo intense ligand-field transitions.

Encouraged by these results, we decided to investigate the use of $\mathbf{1}^+$ as a colorimetric fluoride sensor in protic solvents. Incremental addition of a solution of KF in MeOH to a solution of [**1**]BPh_4 in $MeOH/CH_2Cl_2$ (9/1 v/v) led to the progressive quenching of the band at $\lambda_{max} = 366$ nm and the growth of the low-energy bands at 435 and 487 nm, which correspond to **1**-F (see the Supporting Information, Figure S3). The resulting data was fitted to a 1:1 binding isotherm to afford $K = 5000(\pm 300)\,\text{M}^{-1}$. While attempts to use $\mathbf{1}^+$ in pure water were unsuccessful because of the insolubility of the complex, even at low concentrations, we found that $\mathbf{1}^+$ could be used under biphasic conditions for the detection of ppm concentrations of fluoride anions. Solutions of [**1**]BPh_4 in CH_2Cl_2 (1×10^{-3} M) were layered with aqueous solutions containing 4 ppm (2.0×10^{-4} M TBAF in H_2O, pH 5.2) and 8 ppm (4.0×10^{-4} M TBAF in H_2O, pH 5.3) of fluoride anions. Upon shaking, the organic layers took on the characteristic orange color of **1**-F. The generation of **1**-F was confirmed by UV/Vis and $^{31}P\{^1H\}$ NMR measurements, which showed a conversion of approximately 20% and 35% for [**1**]BPh_4 solutions layered with aqueous solutions containing 4 ppm and 8 ppm of fluoride anions, respectively (see the Supporting Information, Figures S3 and S4). No color change was observed in the presence of common interferents, including Cl^-, Br^-, OAc^-, NO_3^-, and $H_2PO_4^-$, thus indicating that this new sensor is highly selective for fluoride anions. We have also tested the pH tolerance of this sensor and observed that the $^{31}P\{^1H\}$ NMR spectra of solutions of [**1**]BPh_4 (1×10^{-3} M) in CH_2Cl_2 remain unchanged in the pH range of 4–9 (Figure S5). At pH > 9, the ^{31}P NMR resonance of $\mathbf{1}^+$ loses intensity and ultimately disappears. This observation signals the onset of a reaction with hydroxide ions, the product of which has not been identified. Finally, we note that $\mathbf{1}^+$ also captures fluoride anions at pH 9, thus pointing to the tolerance of this new sensor to basic pH (Figure S6).

In summary, we report a cationic trisphosphanylstibine–palladium complex ($\mathbf{1}^+$), which acts as a water-compatible fluoride anion sensor. The sensing properties of this complex result from the formation of a hypervalent fluorostiboranyl motif coupled with a coordination geometry change of the palladium center from square-planar to trigonal-bipyramidal. These structural changes are accompanied by the appearance of intense ligand-field transitions, thus providing a photophysical response for the anion binding event.

Experimental Section

General considerations. **Antimony compounds are highly toxic and should be handled cautiously.** $(o\text{-}(Ph_2P)C_6H_4)_3Sb$[6a] and $[PdCl_2(cod)]$[14] were prepared according to reported procedures. All preparations were carried out without any precautions to exclude oxygen. Solvents were dried by passing through an alumina column (pentane and CH_2Cl_2) or heating to reflux under N_2 over Na/K (Et_2O, *n*-hexane, and THF). All other solvents were used as purchased. KF and TBAF were obtained from Alfa Aesar. Ambient-temperature NMR spectra were recorded on a Varian Unity Inova 400 FT NMR (399.59 MHz for ^1H, 375.99 MHz for ^{19}F, 161.74 MHz for ^{31}P, 100.45 MHz for ^{13}C) spectrometer. Low-temperature ^{31}P NMR spectra were recorded on a Varian Inova 300 FT NMR spectrometer (121.42 MHz for ^{31}P). Chemical shifts (δ) are given in ppm and are referenced against residual solvent signals (^1H, ^{13}C) or external standards ($BF_3{\cdot}Et_2O$ for ^{19}F, and H_3PO_4 for ^{31}P). UV/Vis spectra were recorded on an Ocean Optics USB4000 spectrometer with an Ocean Optics ISS light source. Elemental analyses were performed at Atlantic Microlab (Norcross, GA).

Synthesis of [**1**]BPh_4. A solution of $[PdCl_2(cod)]$ (38 mg, 0.13 mmol) in $CHCl_3$ (2 mL) was added to a solution of $(o\text{-}C_6H_4P(PPh_2))_3Sb$ (122 mg, 0.13 mmol) in $CHCl_3$ (10 mL), and the resulting red solution was stirred for 12 h at room temperature before the solvent was removed in vacuo. The resulting red-orange residue was dissolved in CH_2Cl_2 (2 mL) and a solution of $NaBPh_4$ (44 mg, 0.13 mmol) in EtOH (8 mL) was added dropwise under stirring. A pale-yellow precipitate began to form immediately and the reaction mixture was stirred at room temperature for 2 h. The solid was collected by filtration and washed with EtOH (3 × 2 mL) and Et_2O (3 × 2 mL) to afford [**1**]BPh_4 (143 mg, 90%). Single crystals of [**1**]BPh_4 suitable for X-ray diffraction were obtained by vapor diffusion of Et_2O into a solution of the compound in $CHCl_3$. ^1H NMR (399.59 MHz; $CDCl_3$): $\delta = 6.79$ (t, 4H, BPh, $^3J_{H\text{-}H} = 7.14$ Hz), 6.94 (t, 8H, BPh, $^3J_{H\text{-}H} = 7.33$ Hz), 7.12 (m, 12H, *meta*-PPh), 7.20 (pseudo t, 12H, *ortho*-PPh, $^3J_{H\text{-}H} = 7.59$ Hz), 7.26–7.36 (m, 6H *o*-P(Sb)C_6H_4 + 6H *para*-PPh), 7.40 (m, 8H, BPh), 7.45 (t, 3H, *o*-P(Sb)C_6H_4, $^3J_{H\text{-}H} =$

7.51 Hz), 7.51 ppm (d, 3H, *o*-P(Sb)C_6H_4, $^3J_{H\text{-}H}$ = 7.51 Hz). $^{13}C\{^1H\}$ NMR (100.45 MHz; $CDCl_3$): δ = 121.54 (s), 125.42 (m), 129.03 (s), 129.27 (m), 131.30 (s), 133.25 (m), 135.52 (bs), 136.33 (s), 139.6 (bm), 164.25 ppm (q, J = 49.59 Hz), (four *ipso*-C signals not observed). $^{31}P\{^1H\}$ NMR (161.74 MHz; $CDCl_3$): δ = 39.72 ppm (s). ^{11}B NMR (128.2 MHz; $CDCl_3$): δ = −6.75 ppm (s). Elemental analysis calculated (%) for $C_{78}H_{62}BClPdP_3Sb + 2\,CHCl_3$: C, 59.85 H, 4.02; found C, 59.96; H 3.95.

Synthesis of **1**-F. A solution of [**1**]BPh_4 (50 mg, 0.036 mmol) in $CHCl_3$/MeOH (1:1, 2 mL) was treated with a solution of KF (4 mg, 0.069 mmol) in MeOH (1 mL), which resulted in the immediate formation of an orange precipitate. The precipitate was filtered and washed with MeOH (3 × 2 mL) and Et_2O (3 × 2 mL) to afford **1**-F (38 mg, 97%). Single crystals of **1**-F suitable for X-ray diffraction were obtained by slow vapor diffusion of Et_2O into a solution of the compound in $CHCl_3$. **1**-F could also be prepared in situ by the addition of TBAF (1 equiv) to a solution of [**1**]BPh_4 in $CHCl_3$ or CH_2Cl_2. Multinuclear NMR experiments confirmed quantitative conversion to the fluorostiborane species. Data for **1**-F: ^1H NMR (399.59 MHz; $CDCl_3$): δ = 6.88 (d, 3H, *o*-P(Sb)C_6H_4, $^3J_{H\text{-}H}$ = 7.32 Hz), 7.03 (t, 12H, PPh, $^3J_{H\text{-}H}$ = 7.51 Hz), 7.09–7.15 (m, 6H PPh + 3H *o*-P(Sb)C_6H_4), 7.21–7.29 (m, 12H PPh + 3H *o*-P(Sb)C_6H_4), 8.29 ppm (d, 3H, *o*-P(Sb)C_6H_4, $^3J_{H\text{-}H}$ = 7.87 Hz). $^{13}C\{^1H\}$ NMR (100.45 MHz; $CDCl_3$): δ = 127.83 (m), 129.11 (s), 129.75 (s), 130.28 (s), 132.55 (s), 133.49 (m), 133.65 (m), 136.03 (m), 138.88 (q, J = 10.69 Hz), 148.41 ppm (m). $^{31}P\{^1H\}$ NMR (161.74 MHz; $CDCl_3$): δ = 41.90 ppm (d, $^3J_{F\text{-}P}$ = 20.66 Hz). ^{19}F NMR (375.97 MHz; $CDCl_3$): δ −129.72 ppm (q, $^3J_{F\text{-}P}$ = 20.66 Hz). Elemental analysis calculated (%) for $C_{54}H_{42}FClPdP_3Sb$: C, 60.82 H, 3.97; found C, 59.48; H 3.91.

Biphasic fluoride capture with [**1**]BPh_4. Solutions of [**1**]BPh_4 in CH_2Cl_2 (1.0 mL, 1×10^{-3} M) were layered and shaken with aqueous solutions containing 4 ppm (10 mL, 2.0×10^{-4} M TBAF in H_2O) or 8 ppm (10 mL, 4.0×10^{-4} M TBAF in H_2O) of fluoride anions, which resulted in an immediate color change of the organic layers from yellow to orange. After separation of the layers, 150 μL aliquots of the CH_2Cl_2 layer were diluted to a total volume of 3 mL to provide an approximately 5.0×10^{-5} M solution based on the starting concentration of [**1**]BPh_4. The UV/Vis spectra of these solutions were recorded and showed the appearance of absorption bands in the 400–550 nm range, thus indicating the formation of **1**-F (Figure S3). Layering experiments carried out with distilled water or aqueous solutions of TBACl, TBABr, NaOAc, NaH_2PO_4, or $NaNO_3$ (2.0×10^{-4} M) showed no visible color changes of the CH_2Cl_2 layers. The $^{31}P\{^1H\}$ NMR spectra of [**1**]BPh_4 in CH_2Cl_2 layered with fluoride ion containing solutions showed the appearance of a resonance corresponding to **1**-F (δ = 42.9, d, $^3J_{P\text{-}F}$ = 20.5 Hz) along with a signal corresponding to remaining [**1**]BPh_4 (δ = 39.7). Integration of these signals indicated 20% conversion to **1**-F for the sample layered with a solution containing 4 ppm fluoride ions and 35% for the sample layered with a solution containing 8 ppm fluoride ions (Figure S4).

Received: September 2, 2011
Revised: October 24, 2011
Published online: November 24, 2011

Keywords: antimony · fluoride sensing · hypervalence · Lewis acids · palladium

[1] a) S. Yamaguchi, A. Wakamiya, *Pure Appl. Chem.* **2006**, *78*, 1413–1424; b) Z. M. Hudson, S. Wang, *Acc. Chem. Res.* **2009**, *42*, 1584–1596; c) T. W. Hudnall, C.-W. Chiu, F. P. Gabbaï, *Acc. Chem. Res.* **2009**, *42*, 388–397; d) C. R. Wade, A. E. J. Broomsgrove, S. Aldridge, F. P. Gabbaï, *Chem. Rev.* **2010**, *110*, 3958–3984; e) F. Jäkle, *Chem. Rev.* **2010**, *110*, 3985–4022.

[2] a) S. Yamaguchi, S. Akiyama, K. Tamao, *J. Am. Chem. Soc.* **2000**, *122*, 6793–6794; b) A. C. Tagne Kuate, G. Reeske, M. Schurmann, B. Costisella, K. Jurkschat, *Organometallics* **2008**, *27*, 5577–5587; c) H. Zhao, F. P. Gabbaï, *Nat. Chem.* **2010**, *2*, 984–990.

[3] a) L. H. Bowen, R. T. Rood, *J. Inorg. Nucl. Chem.* **1966**, *28*, 1985–1990; b) M. Jean, *Anal. Chim. Acta* **1971**, *57*, 438–439; c) C. R. Wade, F. P. Gabbaï, *Organometallics* **2011**, *30*, 4479–4481.

[4] a) W. Levason, G. Reid, *Coord. Chem. Rev.* **2006**, *250*, 2565–2594; b) W. Levason, C. A. McAuliffe, *Acc. Chem. Res.* **1978**, *11*, 363–368.

[5] L. Baracco, C. A. McAuliffe, *J. Chem. Soc. Dalton Trans.* **1972**, 948–951.

[6] a) B. R. Higginson, C. A. McAuliffe, L. M. Venanzi, *Inorg. Chim. Acta* **1971**, *5*, 37–40; b) C. R. Wade, F. P. Gabbaï, *Angew. Chem.* **2011**, *123*, 7507–7510; *Angew. Chem. Int. Ed.* **2011**, *50*, 7369–7372.

[7] CCDC 841742 ([**1**]BPh_4), 841743 (**1**-F), 841744 ([**2**]BPh_4), and 841745 (**2**-F) contain the supplementary crystallographic data for this paper. These data can be obtained free of charge from The Cambridge Crystallographic Data Centre via www.ccdc.cam.ac.uk/data_request/cif.

[8] V. V. Sharutin, O. K. Sharutina, A. P. Pakusina, S. A. Smirnova, M. A. Pushilin, *Russ. J. Coord. Chem.* **2005**, *31*, 108–114.

[9] a) W. Malisch, P. Panster, *Angew. Chem.* **1974**, *86*, 708–709; *Angew. Chem. Int. Ed. Engl.* **1974**, *13*, 670–672; b) W. Malisch, H. A. Kaul, E. Gross, U. Thewalt, *Angew. Chem.* **1982**, *94*, 554; *Angew. Chem. Int. Ed. Engl.* **1982**, *21*, 549–550; c) Y. Yamamoto, M. Okazaki, Y. Wakisaka, K.-Y. Akiba, *Organometallics* **1995**, *14*, 3364–3369; d) K. Toyota, Y. Yamamoto, K.-Y. Akiba, *Chem. Lett.* **1999**, 783–784; e) K. Toyota, Y. Yamamoto, K.-Y. Akiba, *Organometallics* **2000**, *19*, 5134–5142; f) K. Toyota, Y. Wakisaka, Y. Yamamoto, K.-Y. Akiba, *Organometallics* **2000**, *19*, 5122–5133; g) C. R. Wade, T.-P. Lin, R. C. Nelson, E. A. Mader, J. T. Miller, F. P. Gabbaï, *J. Am. Chem. Soc.* **2011**, *133*, 8948–8955; h) T.-P. Lin, C. R. Wade, L. M. Pérez, F. P. Gabbaï, *Angew. Chem.* **2010**, *122*, 6501–6504; *Angew. Chem. Int. Ed.* **2010**, *49*, 6357–6360.

[10] a) G. Parkin, *Organometallics* **2006**, *25*, 4744–4747; b) A. F. Hill, *Organometallics* **2006**, *25*, 4741–4743; c) F. G. Fontaine, J. Boudreau, M. H. Thibault, *Eur. J. Inorg. Chem.* **2008**, 5439–5454; d) H. Braunschweig, R. D. Dewhurst, A. Schneider, *Chem. Rev.* **2010**, *110*, 3924–3957; e) A. Amgoune, D. Bourissou, *Chem. Commun.* **2011**, *47*, 859–871; f) G. Bouhadir, A. Amgoune, D. Bourissou, *Adv. Organomet. Chem.* **2010**, *58*, 1–107; g) C. Tsay, N. P. Mankad, J. C. Peters, *J. Am. Chem. Soc.* **2010**, *132*, 13975–13977.

[11] a) J. Wagler, E. Brendler, *Angew. Chem.* **2010**, *122*, 634–637; *Angew. Chem. Int. Ed.* **2010**, *49*, 624–627; b) J. Wagler, A. F. Hill, T. Heine, *Eur. J. Inorg. Chem.* **2008**, 4225–4229; c) P. Gualco, M. Mercy, S. Ladeira, Y. Coppel, L. Maron, A. Amgoune, D. Bourissou, *Chem. Eur. J.* **2010**, *16*, 10808–10817; d) P. Gualco, T.-P. Lin, M. Sircoglou, M. Mercy, S. Ladeira, G. Bouhadir, L. M. Pérez, A. Amgoune, L. Maron, F. P. Gabbaï, D. Bourissou, *Angew. Chem.* **2009**, *121*, 10076–10079; *Angew. Chem. Int. Ed.* **2009**, *48*, 9892–9895; e) J. Grobe, N. Krummen, R. Wehmschulte, B. Krebs, M. Lage, *Z. Anorg. Allg. Chem.* **1994**, *620*, 1645–1658.

[12] a) J. M. Solar, M. A. Ozkan, H. Isci, W. R. Mason, *Inorg. Chem.* **1984**, *23*, 758–764; b) D. A. Roberts, W. R. Mason, G. L. Geoffroy, *Inorg. Chem.* **1981**, *20*, 789–796.

[13] a) S.-I. Aizawa, T. Iida, S. Funahashi, *Inorg. Chem.* **1996**, *35*, 5163–5167; b) W. J. Louw, D. J. A. Dewaal, G. J. Kruger, *J. Chem. Soc. Dalton Trans.* **1976**, 2364–2368; c) J. W. Dawson, H. B. Gray, J. E. Hix, J. R. Preer, L. M. Venanzi, *J. Am. Chem. Soc.* **1972**, *94*, 2979–2987.

[14] D. Drew, J. R. Doyle, *Inorg. Synth.* **1990**, *28*, 346–349.

